

Spliceostatin A targets SF3b and inhibits both splicing and nuclear retention of pre-mRNA

Daisuke Kaida¹, Hajime Motoyoshi², Etsu Tashiro^{1,8}, Takayuki Nojima³, Masatoshi Hagiwara³, Ken Ishigami², Hidenori Watanabe², Takeshi Kitahara^{2,8}, Tatsuhiko Yoshida⁴, Hidenori Nakajima⁵, Tokio Tani⁶, Sueharu Horinouchi⁴ & Minoru Yoshida^{1,4,7}

The removal of intervening sequences from transcripts is catalyzed by the spliceosome, a multicomponent complex that assembles on the newly synthesized pre-mRNA. Pre-mRNA translation in the cytoplasm leads to the generation of aberrant proteins that are potentially harmful. Therefore, tight control to prevent undesired pre-mRNA export from the nucleus and its subsequent translation is an essential requirement for reliable gene expression. Here, we show that the natural product FR901464 (**1**) and its methylated derivative, spliceostatin A (**2**), inhibit *in vitro* splicing and promote pre-mRNA accumulation by binding to SF3b, a subcomplex of the U2 small nuclear ribonucleoprotein in the spliceosome. Importantly, treatment of cells with these compounds resulted in leakage of pre-mRNA to the cytoplasm, where it was translated. Knockdown of SF3b by small interfering RNA induced phenotypes similar to those seen with spliceostatin A treatment. Thus, the inhibition of pre-mRNA splicing during early steps involving SF3b allows unspliced mRNA leakage and translation.

Protein-coding sequences (exons) in primary transcripts are interrupted by intervening sequences (introns) that are eliminated from the pre-mRNA by splicing in the nucleus¹. Splicing occurs by two sequential transesterification reactions^{2,3}. First, the 2' hydroxyl group of the branchpoint adenosine that is located upstream of the 3' end of the intron attacks the 5' splice junction, forming a branched linkage and producing a lariat structure. In the second step, the newly released 3' hydroxyl of the 5' exon attacks the 3' splice junction, thereby forming a new phosphodiester bond between the 5' and 3' exons. Thus, the products of the second step are the ligated exons and the free intron. The precise excision of introns from pre-mRNA is carried out by a multiprotein complex known as the spliceosome^{1,4}. The spliceosome comprises over 150 proteins and five small nuclear RNAs (snRNAs)—U1, U2, U4, U5 and U6—that form the catalytic core of the splicing reaction. The first specific step of spliceosome assembly includes three binding events: the U1 small nuclear ribonucleoprotein (snRNP) binds to the 5' end of the intron (5' splice site)^{5,6}, splicing factor-1 (SF1) binds to the branchpoint sequence⁷, and the U2 snRNP auxiliary factor (U2AF) binds to the polypyrimidine tract located between the branchpoint and the 3' splice site⁸. Next, SF1 is displaced from the pre-mRNA by the ATP-dependent entry of the U2 snRNP, whose SAP155 protein subunit in the SF3b subcomplex interacts with U2AF, followed by the integration of the U4/U6–U5 tri-snRNP

complex^{9–12}. The conformation of this complex is changed to form the catalytically competent spliceosome, from which the U1 and U4 snRNPs are released¹³. After the first chemical splicing reaction to execute the 5' splice site cleavage and lariat formation, further structural rearrangements for the 3' splice site cleavage and exon ligation take place^{1,13}.

Because introns often contain termination codons in frame with the upstream protein coding sequences, leakage of unspliced pre-mRNA into the cytoplasm can result in the production of aberrant, truncated, and potentially deleterious proteins. Therefore, there are several systems to prevent pre-mRNA from being exported to the cytoplasm and translated. For example, *Saccharomyces cerevisiae* Mlp1 functions as a guard to retain pre-mRNA in the nucleus¹⁴. The nonsense-mediated decay (NMD) pathway degrades mRNA species containing a premature termination codon (PTC)¹⁵. Finally, the retention and splicing (RES) complex, which binds to the SF3b subcomplex in the U2 snRNP, has been implicated in pre-mRNA retention in the nucleus^{16,17}. These mechanisms ensure the exclusive translation of mature mRNA in the cytoplasm.

The natural product FR901464 (**Fig. 1a**) was isolated from the fermentation broth of the bacterium *Pseudomonas* sp. as an anticancer compound that enhances the transcriptional activity of the SV40 promoter¹⁸ and causes cell cycle arrest at the G1 and G2/M phases¹⁹.

¹Chemical Genetics Laboratory, RIKEN, 2-1 Hirosawa, Wako, Saitama 351-0198, Japan. ²Department of Applied Biological Chemistry, The University of Tokyo, 1-1-1 Yayoi, Bunkyo-ku, Tokyo 113-8657, Japan. ³Department of Functional Genomics, Medical Research Institute, Tokyo Medical and Dental University, 1-5-45 Yushima, Bunkyo-ku, Tokyo 113-8510, Japan. ⁴Department of Biotechnology, The University of Tokyo, 1-1-1 Yayoi, Bunkyo-ku, Tokyo 113-8657, Japan. ⁵Drug Discovery Research, Fermentation Research Laboratories, Astellas Pharma Inc. 5-2-3 Tokodai, Tsukuba, Ibaraki 300-2698, Japan. ⁶Department of Biological Sciences, Graduate School of Science and Technology, Kumamoto University, 2-39-1 Kurokami, Kumamoto 860-8555, Japan. ⁷Japan Science and Technology Corporation, CREST Research Project, Kawaguchi, Saitama 332-0012, Japan. ⁸Present addresses: Department of Bioscience and Informatics, Faculty of Science and Technology, Keio University, 3-14-1 Hiyoshi, Kohoku-ku, Yokohama 223-8522, Japan (E.T.); Laboratory of Natural Product Chemistry Center for Basic Research, The Kitasato Institute, 5-9-1 Shirokane, Minato-ku, Tokyo 108-8642, Japan (T.K.). Correspondence should be addressed to M.Y. (yoshidam@riken.jp).

Received 28 February; accepted 25 June; published online 22 July 2007; doi:10.1038/nchembio.2007.18

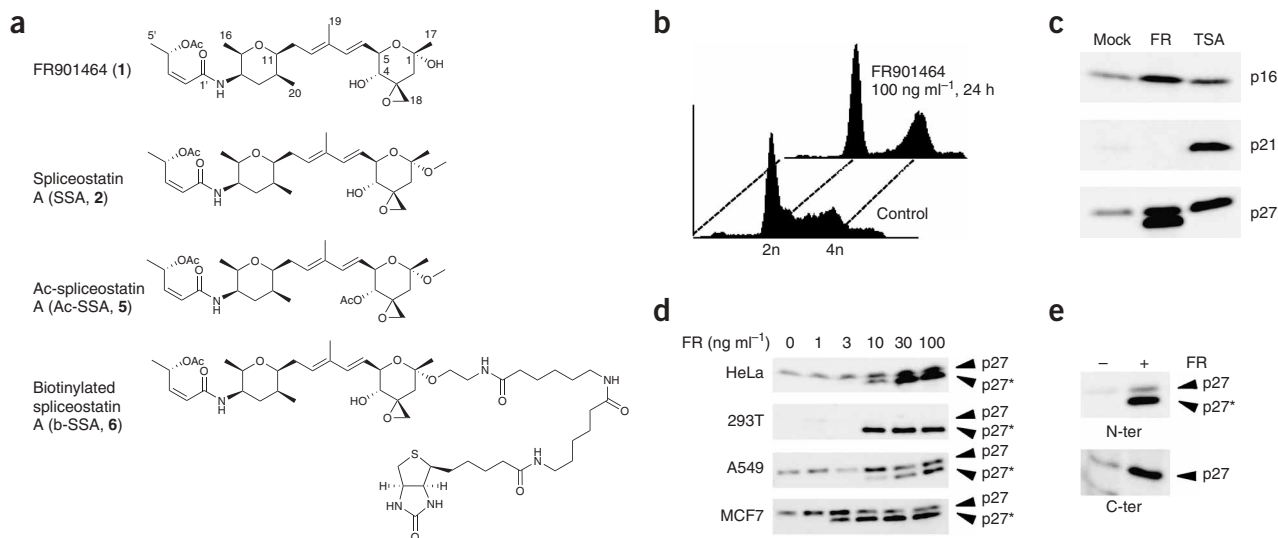


Figure 1 FR901464-induced accumulation of p27*. (a) Structures of FR901464, SSA, Ac-SSA and b-SSA. (b) Flow cytometric profiles of HeLa cells treated with or without FR901464 (100 ng ml⁻¹, 24 h). (c) Detection of CDK inhibitors in the extract of HeLa cells treated with FR901464 (100 ng ml⁻¹, 16 h) or TSA (1 μM, 24 h) using anti-p16, anti-p21, and anti-p27 antibodies. (d) Immunoblotting of p27* in various cell lines treated with the indicated concentration of FR901464 for 14 h. (e) Western blotting of p27 in HeLa cells treated with 100 ng ml⁻¹ of FR901464 for 14 h using an anti-C terminus or an anti-N terminus antibody against p27.

FR901464 showed not only potent cytotoxic activity against a number of different human solid tumor cell lines with half-maximal inhibitory concentration (IC₅₀) values in the low nanomolar range, but also the ability *in vivo* to prolong the life of tumor-bearing mice^{18,19}. Despite its high potency in inducing viral gene promoters, FR901464 paradoxically reduces the mRNA levels of several endogenous genes, including c-Myc¹⁹. Some of the phenotypic changes observed in cells treated with FR901464 were found to be similar to those of known histone deacetylase inhibitors, such as trichostatin A (3). However, analysis of the acetylation state of the isolated histones indicated that FR901464 is not an inhibitor of histone deacetylase (HDAC) activity²⁰. This unprecedented pharmacological profile of FR901464 has drawn considerable interest, prompting us to further investigate its mechanism of action. In this report, we present evidence that FR901464 and its methylated derivative spliceostatin A (SSA) inhibit pre-mRNA splicing by binding noncovalently to the SF3b subcomplex in the U2 snRNP. Furthermore, our results uncover a surprising ability of spliceostatin A to leak pre-mRNA to the cytoplasm, thereby allowing translation of unspliced mRNAs.

RESULTS

FR901464 produces a C-terminally truncated p27

To gain insight into the mechanism by which FR901464 arrests the cell cycle in the G1 and G2/M phases (Fig. 1b), we tested its effect on the expression of several cell cycle regulators in HeLa cells. Progression of the cell cycle is strictly regulated by a number of regulatory proteins, including cyclins and cyclin-dependent protein kinases (CDKs). CDKs generate the major driving force, acting as the cell cycle engine, and their activity is controlled by their association with positive and negative regulatory proteins and multiple post-translational modifications. For instance, CDK2 is activated upon associating with cyclin E or A, whereas CDK4 and CDK6 are activated by D-type cyclins²¹. CDK activity is negatively regulated by direct interactions with proteins referred to as CDK inhibitors. p21 and p27, members of this family of proteins, both block the transition from G1 to S phase

by binding to the CDK2 complex^{22,23}. On the other hand, p16, one of the INK4-family proteins, serves as a negative regulator for the D-type cyclin-dependent kinases²⁴. To investigate the effect of FR901464 on these factors, we first determined the cellular levels of these cell-cycle regulatory proteins by western blotting. Of the proteins tested, the expression of cyclin A and CDKs was essentially unchanged by FR901464 (Supplementary Fig. 1a online), whereas that of the p16 and p27 CDK inhibitors was upregulated. In contrast, the expression of p21 was increased by the HDAC inhibitor trichostatin A (Fig. 1c). Notably, a truncated form of p27 also accumulated in the FR901464-treated cells. We named this variant p27*. Although the absolute expression level of p27 varied, we consistently observed p27* accumulation in all the human cell lines tested (Fig. 1d). Next, we determined the portion of p27 that is absent in p27* using two distinct anti-p27 antibodies raised against the N- and C-terminal peptides of p27. Whereas the former antibody reacted with p27*, the latter did not (Fig. 1e), which suggests that p27* is a C-terminally truncated form of p27. Although p27 is known to be degraded by the 26S proteasome²⁵, p27* was not a proteasomal degradation product; treatment with the proteasome inhibitor MG132 (4) did not reduce the amount of p27* (Supplementary Fig. 2a online). Furthermore, p27* could not be generated from p27 complementary DNA expression in cells treated with FR901464, which indicates that it is not the product of proteolytic processing (Supplementary Fig. 2b).

Identification of SF3b as the target protein

As a result of total synthesis and derivatization of FR901464, we previously reported that its methyl ketal derivative (Fig. 1a) is fully active²⁶. It was even more stable than FR901464 (Supplementary Fig. 3a online), probably because of the chemical stability of the methylketal group compared with the hemiketal group^{27,28}. Indeed, the methylketal derivative induced p27* production (Fig. 2a) at low concentrations similar to those observed for FR901464. We named the methylketal derivative spliceostatin A based on its mechanism of action (see below) and used it for further studies. In contrast, the

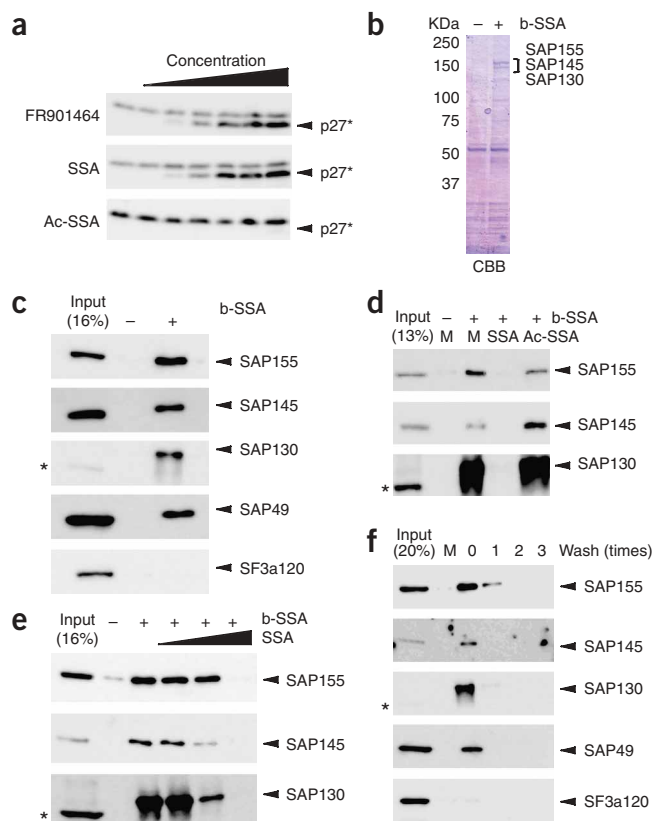


Figure 2 Identification of the splicing factor SF3b as the target.

(a) Detection of p27* in HeLa cells treated for 14 h with compounds at concentrations of 1, 3, 10, 30, 100 and 300 ng ml⁻¹, which correspond respectively to 2, 6, 20, 59, 200 and 590 nM for FR901464, 1.9, 5.8, 19, 58, 190 and 580 nM for SSA and 1.8, 5.3, 18, 53, 180 and 530 nM for Ac-SSA. (b) Purification of SSA-binding proteins from HeLa cell extract (1 mg total protein, 500 μl) using biotinylated SSA (2 μM) and streptavidin beads. The proteins were subjected to SDS-PAGE and stained with Coomassie Brilliant Blue. (c) Detection of specific binding to SF3b components by biotinylated SSA. Proteins bound to biotinylated SSA (2 μM) in HeLa cell extract (300 mg total protein, 150 ml) were isolated using streptavidin beads. SF3b components were detected using anti-SAP155, anti-SAP145, anti-SAP130, anti-SAP49 and anti-SF3a120 antibodies. (d,e) Competition assay. Cell extracts (300 μg total protein, 150 μl) that had been preincubated with 950 nM SSA (d), 900 nM Ac-SSA (d), or 0.95, 9.5 and 95 nM SSA (e) were incubated with 2.5 μM (d) or 5 μM (e) biotinylated SSA, and the binding proteins were detected by western blotting. (f) Immunoblotting of the SF3b components after washing with an SDS-containing buffer. SSA-binding proteins that had been washed with IP buffer containing 0.025% SDS were subjected to western blotting. Asterisks indicate a nonspecific band (c-f).

derivative acetylated at the C4 hydroxyl group (Ac-spliceostatin A, 5) (Fig. 1a) was inactive at least up to 500 nM (Fig. 2a). The biotinylated derivative of spliceostatin A (6) (Fig. 1a) was biologically active (Supplementary Fig. 3b), although its *in vivo* activity was about 20-fold weaker than that of spliceostatin A. Using the active biotinylated probe, we searched for proteins that specifically bound to spliceostatin A. As a result, proteins with molecular sizes between 130 and 160 kDa were detected by SDS-PAGE followed by Coomassie staining (Fig. 2b). LC-MS/MS analysis revealed that these proteins were SAP155, SAP145 and SAP130, all of which are known as components of the SF3b splicing subcomplex in the U2 snRNP⁴. We confirmed the endogenous binding of SSA to the SF3b complex by western blotting of bead-bound proteins using anti-SAP155, anti-SAP145, anti-SAP130 and

anti-SAP49 antibodies under the high-salt conditions that dissociate the SF3b complex from the U2 snRNP⁴ (Fig. 2c). On the other hand, another spliceosome subcomplex, SF3a, was not detected in the SSA-bound fraction. To test the specificity of the SF3b complex binding, we carried out a competition experiment using SSA and Ac-SSA as the competitors. Whereas binding was completely lost upon addition of excess SSA, the biologically inactive Ac-SSA did not inhibit binding (Fig. 2d), which indicates that SSA's binding to SF3b is specific. A titration experiment indicated that compared with biotinylated SSA, 50 times less SSA is sufficient to compete with biotinylated SSA for its binding to the SF3b complex (Fig. 2e). Because FR901464 and SSA both contain a highly reactive epoxide group in the right-handed pyran ring, we assumed that SF3b is covalently bound to biotinylated SSA through this epoxide moiety. However, the ability of SF3b proteins to be readily removed from the beads by washing with SDS-containing buffer made this binding mechanism unlikely (Fig. 2f).

Spliceostatin A inhibits *in vitro* and *in vivo* splicing

Next, we examined the biological consequences of SSA binding to SF3b. Because SF3b has an important role in the U2 snRNP, which binds to the mRNA branchpoint sequence^{9,12}, we first tested the effect of SSA on the splicing reaction *in vitro*. *In vitro*-transcribed pre-mRNAs encoding β-globin and IgM were purified and incubated

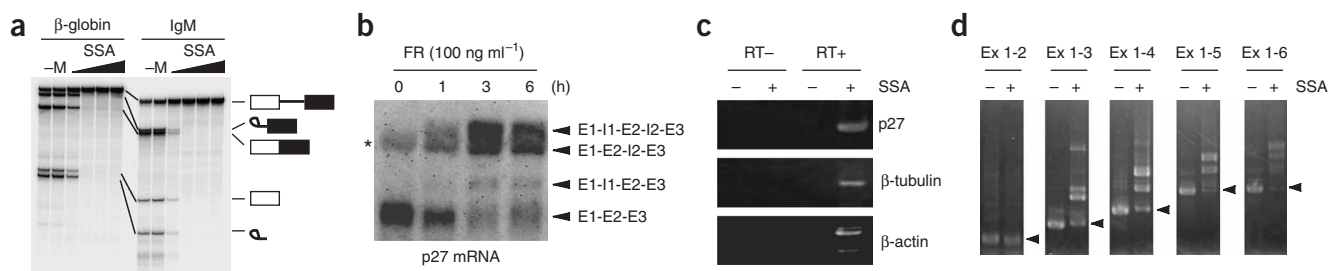


Figure 3 SSA-mediated inhibition of *in vitro* and *in vivo* splicing. (a) *In vitro* splicing. Radio-labeled β-globin or IgM pre-mRNAs were incubated with nuclear extract⁴⁸ that was preincubated with water (-), MeOH (M) or SSA (19, 58, 95 and 190 nM) at 4 °C for 1 h. RNAs were separated by Urea-PAGE and detected by autoradiography. The bands corresponding to the pre-mRNA, spliced product, and intermediates are depicted by symbols. (b) Northern blotting of p27 mRNA prepared from HeLa cells treated with FR901464 (100 ng ml⁻¹) for the indicated times. (c,d) RT-PCR using RNAs prepared from cells treated with SSA (100 ng ml⁻¹, 6 h) or MeOH. Primer sets used in c were those for annealing exon 1 and intron 1 of p27, intron 2 and exon 4 of β-tubulin, and exon 3 and intron 4 of β-actin, respectively. RT+ and RT- show samples with or without reverse transcription. Primer sets used in d were those for annealing exon 1 and exon 2-6, respectively. Arrowheads represent mature mRNAs.

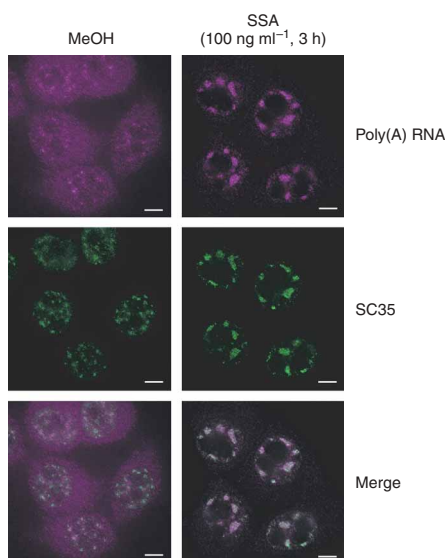


Figure 4 Subcellular localization of poly(A) RNA and SC35. After HeLa cells had been treated with SSA (100 ng ml⁻¹, 3 h) or MeOH, the localization of poly(A) RNA and SC35 were visualized using a digoxigenin-labeled oligo-dT probe and an anti-SC35 antibody, respectively. Scale bars, 5 μm.

with nuclear extract. This reaction resulted in the formation of mature mRNA and intron-containing sequences as described previously^{29,30}. However, in the presence of SSA, the splicing reaction was blocked in a dose-dependent manner, which clearly indicates that SSA inhibits *in vitro* splicing (Fig. 3a). Next, we evaluated the effect of SSA on splicing *in vivo* using a plasmid harboring a similar β-globin construct with a single intron. When the cells transfected with the plasmid were treated with SSA for 12 h, a marked decrease in the mature transcript and an increase in pre-mRNA were detected upon RT-PCR analysis (Supplementary Fig. 4a online). To complement our analysis of splicing of plasmid-derived gene transcripts, we also used p27 mRNA to examine the effect on splicing of endogenous gene transcripts (Fig. 3b). Northern blot analysis of p27 mRNA in cells treated with FR901464 showed that both mRNA species containing several combinations of exons/introns and pre-mRNA accumulated, whereas the amount of mature mRNA decreased (Fig. 3b). This effect was not limited to the p27 gene. RT-PCR using primers designed for the detection of intron-containing transcripts demonstrated that all transcripts tested in this study, including those encoding β-actin, β-tubulin and IκBα, contained unspliced mRNAs (Fig. 3c,d). Despite its ability to completely inhibit splicing *in vitro*, the inhibitory activity of SSA *in vivo* seemed to be partial. Even at a very high concentration (1 mg ml⁻¹), the mature forms of at least p27 and IκBα transcripts remained (Supplementary Fig. 4b,c).

Figure 5 Pre-mRNA translation in SSA-treated cells. (a) Schematic representation of the p27 mRNA species, p27-int-HA plasmid, and p27 protein species. Green and blue boxes represent coding and noncoding regions, respectively. Red and yellow boxes represent HA and Myc tags, respectively. (b) Detection of intron translation. p27-Myc and p27*-HA in HEK 293T cells transfected with the p27-int-HA plasmid treated with or without SSA (100 ng ml⁻¹) for 14 h were detected by western blotting. (c) Detection of IκBα proteins in HeLa cells treated with SSA at 100 ng ml⁻¹ for 16 h. IκBα*, IκBα** and IκBα*** indicate truncated forms of IκBα, which may be translated from pre-mRNA species shown in Supplementary Figure 4c.

Effects on mRNA export and spliceosome morphology

Splicing is required for the efficient transport of mRNA³¹; therefore, we next examined whether SSA treatment affects the subcellular distribution of mRNA. *In situ* hybridization of poly(A) RNA showed that a large population of mRNA species are distributed in the cytoplasm in control cells. After 3-h treatment with SSA, however, mRNA was found in a number of nuclear domains, and the cytoplasmic RNA signal was lower (Fig. 4). These results suggest that a fraction of the unspliced mRNA species that accumulate in the SSA-treated cells are retained in the nucleus. The snRNPs and some splicing factors such as SC35 have been demonstrated to be organized in a specific distribution pattern in the nucleus called “speckles.” The speckles are composed of 20–50 irregularly shaped regions in the nucleus, which corresponds to structures previously designated as interchromatin granules and perichromatin fibrils³². It is now thought that the interchromatin granule clusters are the sites of splicing factor storage and/or assembly, whereas the perichromatin fibrils represent the actual nascent pre-mRNA transcripts to which splicing factors from interchromatin granule clusters have moved to carry out splicing³³. The subnuclear localization of SC35-containing speckles was also greatly affected by SSA: the speckles were larger, but less abundant (Fig. 4). These changes are similar to those observed in cells in which SF3a (another U2 snRNP component) was knocked down, or in which oligonucleotides that inhibit pre-mRNA splicing were injected^{32,34}. Furthermore, the mRNA induced by SSA treatment colocalized with SC35 (Fig. 4).

Spliceostatin A treatment allows translation of pre-mRNA

If accumulated unspliced or partly spliced mRNAs are allowed to be exported and translated, proteins containing polypeptides derived from the intron sequences should be generated. The p27 protein translated from pre-mRNA should contain the intron 1-derived sequence but lack the exon 2 portion, because intron 1 has an in-frame termination codon (Fig. 5a). The apparent molecular size of 22 kDa for p27* coincides well with a putative gene product derived from the p27 mRNA species. To test this possibility, we constructed a reporter system named p27-int-HA by inserting an in-frame hemagglutinin (HA) tag sequence before the termination codon in

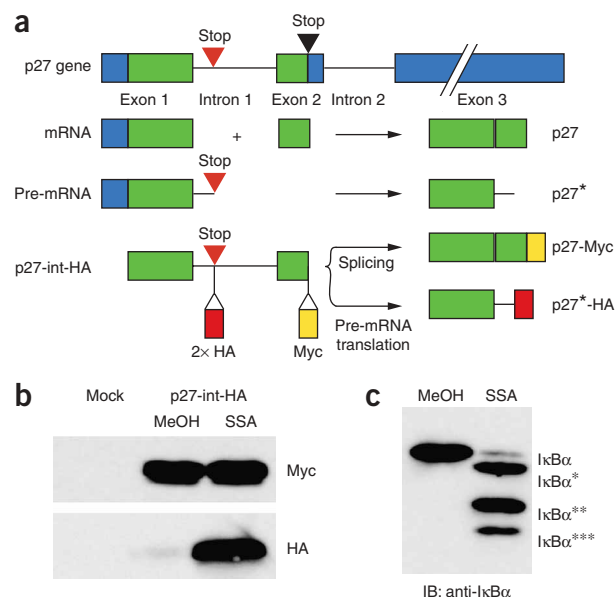
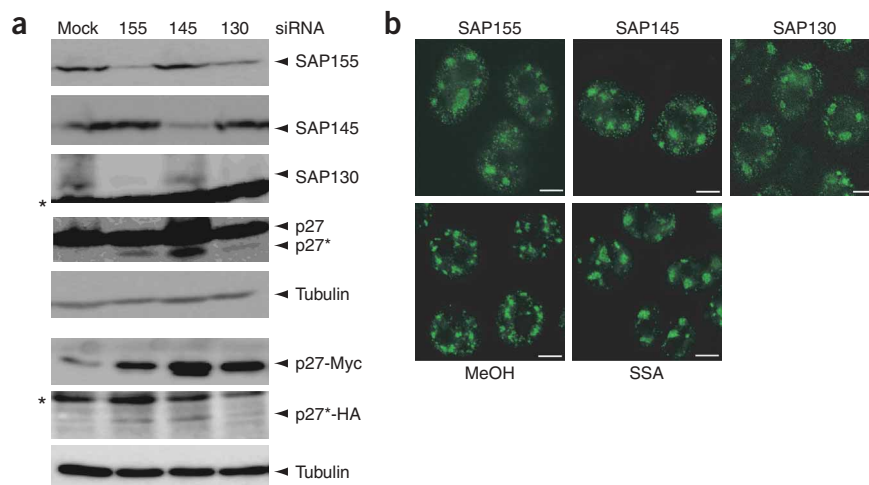


Figure 6 Phenotypic changes induced by SF3b knockdown. **(a)** Translation of unspliced mRNA in SF3b knockdown cells. Production of p27* was detected in HeLa cells transfected with siRNA against SAP155, SAP145 and SAP130 (upper). Cells that had been transfected with the reporter plasmid p27-int-HA were knocked down with siRNA against SAP155, SAP145 and SAP130 (lower). Asterisks indicate a nonspecific band. **(b)** Morphology of SC35 nuclear speckles in SF3b knockdown cells. HeLa cells were transfected with siRNA against SAP155, SAP145 and SAP130, and cultured for 3 d. Scale bars, 5 μ m.



intron 1 and a Myc tag sequence before the termination codon in exon 2 in the gene encoding p27 (Fig. 5a). If the transcript of this reporter gene was correctly spliced, only the Myc sequence should be translated, but if the unspliced mRNA could be translated, the protein containing the intron-derived polypeptide tagged with HA should be produced. Whereas human embryonic kidney (HEK) 293T cells treated with carrier solution not containing SSA produced only the Myc-containing protein, SSA treatment induced cells to generate the HA-tagged protein in addition to the Myc-tagged form (Fig. 5b). These results indicate that in SSA-treated cells, unspliced RNA not only accumulates but is also translated to form p27*. This idea was further supported by the observation that p27* could not be generated from cDNA in cells treated with SSA (Supplementary Fig. 2b). Furthermore, we found several proteins that are reactive with the anti-I κ B α antibody (Fig. 5c); these proteins are likely produced from a variety of the partially spliced mRNAs, detected by RT-PCR (Fig. 3d).

SF3b knockdown causes similar phenotypic changes

To verify that the functional defect in SF3b by SSA can account for the phenotypic changes seen in SSA-treated cells, we analyzed the effects of siRNA directed toward each component of SF3b. The successful knockdown of each component by siRNA was confirmed by western blotting (Fig. 6a) and immunofluorescent staining (Supplementary Fig. 5a,b online). Each siRNA reduced the protein level of SAP155, SAP145 and SAP130. Notably, siRNA against SAP155 also reduced the level of SAP130, and, conversely, siRNA against SAP130 decreased SAP155 levels. Because of their tight association, it seems likely that these two proteins are mutually important in maintaining protein stability³⁵. In all cells treated with siRNA, p27* production was detected (Fig. 6a, upper panel). The level of p27* production was

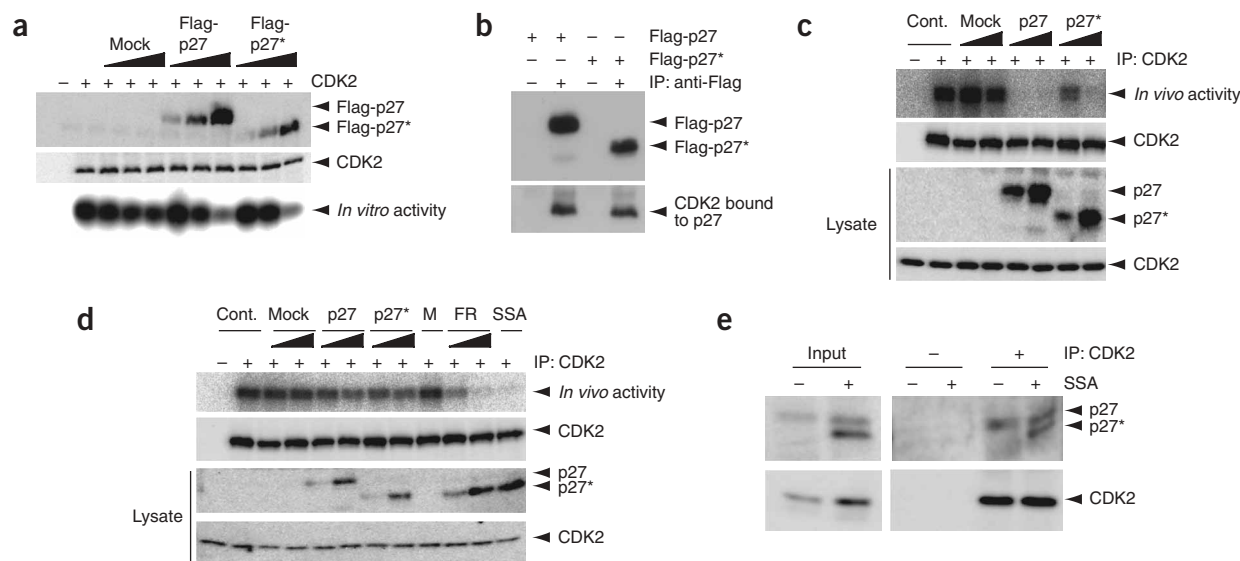


Figure 7 p27* as a functional CDK inhibitor. **(a)** *In vitro* CDK2 kinase activity was analyzed by autoradiography using FLAG-p27 or FLAG-p27* purified from HEK 293T cells, immunoprecipitated CDK2, histone H1, and (γ -³²P)ATP. **(b)** *In vivo* binding of p27* to CDK2. The amount of p27- or p27*-bound endogenous CDK in cells transfected with FLAG-p27 or FLAG-p27* was measured by western blotting. Each 4.5 μ g of plasmid DNA was used for transfection. **(c)** *In vivo* CDK2 kinase assay. The kinase activity in the protein complex containing CDK2 and p27 or p27* was measured by autoradiography, using histone H1 and (γ -³²P)ATP as substrates. The amounts of plasmids used were 0.2 and 0.6 μ g. **(d)** CDK2 kinase activity in drug-treated cells. The kinase activity in HEK 293T cells treated with MeOH, FR901464 (20 and 200 nM) or SSA (190 nM), or in cells transfected with pcDNA3.1-FLAG-p27 or pcDNA3.1-FLAG-p27* was determined with the *in vivo* CDK kinase assay. The amounts of plasmids used were 0.03 and 0.1 μ g. **(e)** *In vivo* binding of p27* to CDK2 in the cells treated with MeOH or SSA.

highest in SAP145 siRNA-treated cells, although the reason is currently unknown. When cotransfected with the p27-int-HA plasmid as a reporter, HA-tagged protein was also detectable in the knockdown cells (Fig. 6a, lower panel). We detected an abnormal distribution of SC35-containing speckles induced by the siRNAs that was similar to that observed in the drug-treated cells (Fig. 6b). These results confirm that both the p27* production and the mislocalization of spliceosomes are results of SF3b inhibition by SSA.

Biological activity of p27*

Finally, we investigated the relevance of the p27* production to the cell cycle arrest induced by FR901464 (Fig. 1b) by expressing p27* cDNA. Because of the presence of the splice site within the sequence for the nuclear localization signal (NLS), p27* has a partial NLS, which may impair its nuclear localization (Supplementary Fig. 6a online). Indeed, p27* was distributed throughout the cell, whereas p27 localized mainly to the nucleus (Supplementary Fig. 6b). Because p27 has been shown to have a functional nuclear export signal³⁶, it should be localized entirely to the cytoplasm if the NLS function were completely abolished. To assess the activity of the p27* NLS, we treated cells expressing p27* with leptomycin B (LMB, 7), a specific nuclear export inhibitor that blocks the CRM1 nuclear export factor³⁷. LMB treatment increased the nuclear localization of p27* (Supplementary Fig. 6b), which suggests that p27* is still shuttling. Next, we analyzed the role of p27* as an active CDK inhibitor. Immunopurified p27*, like full-length p27, inhibited the *in vitro* CDK2 kinase activity in a dose-dependent manner (Fig. 7a). When p27* was expressed in HEK 293T cells, endogenous CDK2 was associated with p27* and with p27 (Fig. 7b), and the *in vivo* kinase activity of the CDK2 complex isolated from the transfected cells was greatly reduced in a manner that was dependent on the expression levels of p27 and p27* (Fig. 7c). These results clearly show that p27* expressed in the cells is active in inhibiting endogenous CDK2. Moreover, we measured the CDK2 kinase activity in drug-treated cells expressing endogenous p27*. The *in vivo* CDK2 activity became almost undetectable as the p27* level increased in cells treated with FR901464 or SSA (Fig. 7d). The p27* protein expressed in the presence of the drug was associated with endogenous CDK2 in cells (Fig. 7e).

DISCUSSION

In 1996, researchers reported the discovery of three new compounds, differing only in the substituents on the right-handed pyran ring, and named them FR901463 (8), FR901464 and FR901465 (9)¹⁸. FR901464 was the most active, although all three compounds showed similar biological activity. Recently, several groups succeeded in the total synthesis of FR901464, and analogs such as meayamycin (10), which lacks the hemiketal functionality, were shown to have more potent activity than the natural product owing to their increased stability^{27,28}. In this study, we demonstrated that spliceostatin A, a stable methylketal derivative of FR901464, is a small-molecule inhibitor of the SF3b splicing factor. It is likely that the splicing inhibition caused the observed morphological changes in the nuclear speckles and partial poly(A) RNA accumulation in these speckles, because it has been reported that *in vivo* splicing inhibition results in reorganization of splicing factors in the nucleus^{32,34} and that mRNA export is coupled to splicing³¹. We suggest calling this family of anticancer compounds that inhibit pre-mRNA splicing 'spliceostatins'.

Previous structure-activity relationship studies have suggested the importance of the right-handed pyran ring for the biological activity of FR901464 (refs. 26–28). Indeed, we showed that acetylation at the C4 position greatly reduces the compound's activity (Fig. 2a). In

particular, introduction of a cyclopropyl group in place of the epoxide resulted in a complete loss of activity, thereby demonstrating its crucial role²⁸. The epoxide moiety has been shown to be highly reactive, and its opening by β -elimination gives two enones, one of which can undergo dehydration to form a furan under physiologically relevant conditions²⁷. We therefore speculated that the epoxide mediates covalent binding to the target protein. However, the binding was reversible, making this unlikely. We were unable to determine the noncovalent binding site of SSA in the present study. It seems possible that SAP130 is the target, because it is the most efficiently enriched protein among the complex components bound to the biotinylated probe (Fig. 2c–f). However, SAP130, as well as SAP145 and SAP49, rapidly dissociated from the complex during washing, whereas SAP155 was more tightly bound to biotinylated SSA and was the last protein to be released (Fig. 2f), which suggests that SAP155 is another candidate protein bound directly to SSA. Further analysis such as binding assays using recombinant proteins, photoaffinity labeling or X-ray crystallography will be needed to elucidate the manner in which SSA binds to SF3b at the molecular level.

The present study suggests that SF3b has a dual function in the splicing and retention of pre-mRNA. It has been shown that pre-mRNA or partially spliced mRNA is retained in the nucleus by mRNA-binding heterogeneous nuclear ribonucleoprotein (hnRNP) particles³⁸. In budding yeast, Mlp1 localized at the nuclear pore prevents the export of pre-mRNA¹⁴. Furthermore, NMD is responsible for the degradation of mRNA species containing PTCs¹⁵. These mechanisms are thought to ensure that only spliced mRNA is transported and translated. Surprisingly, however, nuclear export of unspliced mRNA and accumulation of proteins containing intron-derived sequences occurred during drug treatment. An active p27 CDK inhibitor derivative, p27*, which lacks part of the C-terminal region of p27, was one such protein. It has been reported that the budding yeast protein Msl5, a homolog of the mammalian splicing factor SF1, is involved in pre-mRNA nuclear retention³⁹. The *msl5* mutations resulted in leakage of pre-mRNAs without concomitant splicing inhibition. We also showed that p27*-HA accumulates in SF1 knock-down mammalian cells (Supplementary Fig. 7a online), although SSA does not bind to SF1 (Supplementary Fig. 7b). SF1 and SF3b, both of which bind to the branchpoint^{7,9,40}, may act as markers indicating the existence of an intron, which is recognized by a dedicated 'retention machinery'. The RES complex containing Pml1p, Ist3p and Bud13p, which has been shown to be responsible for nuclear retention of pre-mRNA in yeast, was copurified with SF3b^{16,17}. Yeast two-hybrid data show that association of the RES complex may be linked through the largest SF3b subunit¹⁷. These observations support the idea that SF3b is an important component of the nuclear retention mechanism.

NMD is a highly conserved surveillance mechanism that prevents the synthesis of truncated proteins from mRNA containing PTCs¹⁵. In mammalian cells, NMD is linked to splicing, as the position of the termination codon relative to the last exon-exon junction determines whether it is interpreted as pre-mRNA. Termination codons that are followed by an exon-exon junction positioned >50–55 nucleotides (nt) downstream trigger mRNA degradation by NMD⁴¹. Consistent with this rule, normal stop codons are nearly always found in the last exon, or within 55 nt of the end of the second-to-last exon of the gene⁴¹, and intronless genes containing PTCs are immune to NMD⁴². Despite the presence of PTCs in most introns, the unspliced mRNA species accumulated after splicing inhibition by SSA seem to be very stable. It looks as if NMD is completely bypassed, at least in the cases of p27 and I κ B α , probably because some of the unspliced mRNAs are also immune to NMD. For instance, according to the expected

function of NMD, p27 pre-mRNA (Ex1-In1-Ex2-In2-Ex3) and a partly spliced mRNA (Ex1-Ex2-In2-Ex3) should not be destroyed, but rather another form (Ex1-In1-Ex2-Ex3) should be degraded. In fact, the result shown in **Figure 3b** was consistent with this prediction. In addition, we confirmed that FR901464 does not inhibit the degradation of β -globin mRNA containing PTC, an NMD reporter⁴³, by NMD (**Supplementary Fig. 8** online). We therefore conclude that FR901464 and SSA do not affect NMD.

Because splicing is a fundamental step in eukaryotic gene expression, its inhibition may be generally highly toxic to cells and animals. However, though FR901464 has potent antitumor activity^{18,19}, it is only mildly toxic to animals. The partial inhibition of *in vivo* splicing likely underlies this moderate toxicity, for mature mRNA can still be produced in cells treated with the drug. In addition, there are many genes in which the first exon encodes only a short protein sequence. Because most of the introns contain the in-frame termination codons, proteins expressed from such transcripts should be undetectably short and nondeleterious. Indeed, no truncated forms of cell cycle regulators other than p27 were detected in western blot analysis (**Fig. 1c** and **Supplementary Fig. 1b**). We accidentally found truncated proteins expressed from the gene encoding p27 (5 kb) and the gene encoding I κ B α (3.2 kb), both of which are smaller than the average length of human genes (27 kb)⁴⁴. Although it is still possible that a subset of pre-mRNA is selectively exported by an unknown mechanism, we speculate that long transcripts containing introns cannot be exported efficiently. If so, the production of the active truncated proteins would be limited to a small subset of genes that are short in size but have relatively long coding sequences upstream of their intronic PTCs. In this context, accumulation of active p27* may be important for the growth inhibition of cancer cells by FR901464. It is conceivable that p27* is resistant to proteasomal degradation, because of the lack of the C-terminal phosphorylation site (T187) whose phosphorylation by CDK is required for ubiquitination⁴⁵ (**Supplementary Fig. 6a**). The production of p27* may trigger a circuit of events to arrest the cell cycle by reducing the CDK activity in cycling cancer cells, which may lead to stabilization of endogenous p27 and a further decrease in the CDK activity. Of course, it is highly probable that a variety of phenotypic changes observed in the FR901464-treated cells can be ascribed to the synthesis of truncated proteins other than p27*.

Although the mechanism by which splicing inhibition causes selective killing of tumor cells remains elusive, the SF3b inhibitors may represent a new class of antitumor agents. Furthermore, splicing is essential for infection by a class of viruses, and some are sensitive to SR kinase inhibitors that modulate alternative splicing⁴⁶. Therefore, SF3b may also be a valuable target for antiviral drugs. Thus, spliceostatsins may potentially be used not only as a powerful tool for analyzing mRNA quality control but also as a seed for developing new therapeutics.

METHODS

Materials, cell lines and antibodies. HeLa S3, HEK 293T, MCF7, and A549 cells were cultured in DMEM containing 10% heat-inactivated FBS (Sigma). FR901464 was isolated from the fermentation broth of *Pseudomonas* sp. No.2663 as described previously¹⁸. See **Supplementary Methods** online for characterization of FR901464. SSA and biotinylated SSA were synthesized as described²⁶. See **Supplementary Methods** for characterization of SSA and biotinylated SSA. TSA, MG132 and cycloheximide (**11**) were purchased from Wako Pure Chemical Industries. LMB was described previously⁴⁷. See **Supplementary Methods** for antibodies used in this report.

Synthesis of Ac-SSA. See **Supplementary Methods** for experimental procedures and compound characterization.

Plasmids, siRNA and transfection. See **Supplementary Methods** for plasmid construction. The siGENOME siRNAs for SAP155, SAP145 and SF1 were purchased from GE Healthcare. The siRNA used for SAP130 was 5'-AUACAAU UACCCUAUGUCCUU-3'. HeLa and HEK 293T cells were transiently transfected with each plasmid using the Lipofectamine2000 Reagent (Invitrogen). HeLa cells were transfected with siRNAs using the DharmaFECT 1 Reagent (Dharmacon) according to the manufacturer's instructions.

Flow cytometry. HeLa cells grown in the presence or absence of drugs were washed with phosphate-buffered saline (PBS), trypsinized, harvested and fixed. Cells were resuspended in propidium iodide-containing buffer and subjected to analysis using an EPICS XL System II (Beckman Coulter).

Western blotting. HeLa cells were harvested and sonicated for 10 s twice in an ice-cold (0 °C) IP Buffer (50 mM HEPES-KOH (pH 7.5), 150 mM NaCl, 1 mM EDTA, 2.5 mM EGTA) and a complete protease inhibitor cocktail (Roche). Proteins were separated by SDS-PAGE and stained with Coomassie Brilliant Blue or transferred to a PVDF membrane (Millipore) by electroblotting. After the membranes had been incubated with primary and secondary antibodies, the immune complexes were detected with an Immobilon Western kit (Millipore), and the luminescence was analyzed with a LAS-3000 image analyzer (Fujifilm).

SSA-binding assay. HeLa cell extracts were prepared as mentioned above using 1 M NaCl/IP Buffer (50 mM HEPES-KOH (pH 7.5), 1 M NaCl, 1 mM EDTA, 2.5 mM EGTA). The extracts were mixed with biotinylated SSA and incubated for 6 h at 4 °C. After UltraLink immobilized Streptavidin Plus (PIERCE) had been added, the mixture was further incubated for 1 h at 4 °C. The bound proteins were washed with IP buffer or 0.025% SDS containing IP buffer, boiled in 30 μ l of SDS sample buffer, and subjected to western blotting. For the competition assay, SSA or Ac-SSA was added at various concentrations before incubating with biotinylated SSA.

Mass spectrometry. See **Supplementary Methods** for experimental procedures.

In vitro splicing. The human β -globin (exon 1, 177 nt; intron 1, 130 nt; and exon 2, 148 nt) and IgM (exon C3, 154 nt; intron, 107 nt; and exon C4, 119 nt) pre-mRNA substrates were m7G-capped and ³²P-labeled by *in vitro* transcription. HeLa nuclear extract was preincubated with methanol or SSA for 1 h at 4 °C. The *in vitro* splicing reactions were performed in 20- μ l volumes at 30 °C for 90 min according to the conditions described²⁹. After the reaction, the RNA was subjected to a denaturing PAGE analysis and autoradiography.

Northern blotting. mRNA was prepared with a QuickPrep micro mRNA Purification Kit (Amersham Biosciences) according to the manufacturer's protocol. The probe for detection of p27 mRNA was amplified by PCR using the PCR DIG Probe Synthesis Kit (Roche). Hybridization and detection were carried out using DIG Easy Hyb Granules (Roche), a DIG Wash and Block Buffer Set (Roche) and a DIG Luminescent Detection Kit (Roche) and an LAS-3000 image analyzer (Fujifilm).

RT-PCR. Total RNA was prepared with TRIzol (Invitrogen) according to the manufacturer's instructions. Reverse transcription was carried out using M-MLV Reverse Transcriptase (Promega). See **Supplementary Methods** for primer sets used in RT-PCR.

Immunofluorescence analysis. Cells were fixed with 3% formaldehyde for 10 min at room temperature. After washing with PBS, cells were permeabilized with 1% Triton X-100 for 10 min at room temperature and rinsed with PBS three times. Samples were treated with 5% FBS-containing PBS for 30 min, incubated first with the anti-SC35 or anti-FLAG antibody, and then with the Alexa Fluor 488 goat anti-mouse IgG antibody (Molecular Probes), and finally analyzed with a DeltaVision system (Applied Precision) using an Olympus IX70 fluorescence microscope equipped with an UPlan Apo 100 \times lens.

In situ hybridization. Cells were prepared for fluorescence *in situ* hybridization by fixation with 3% formaldehyde for 15 min at room temperature. After washing with PBS, cells were permeabilized with 0.5% Triton X-100 for 5 min on ice, rinsed with PBS and 2 \times SSC. Hybridization was done at 42 °C in a solution containing 2 \times SSC, 20% formamide, 1 mg ml⁻¹ of tRNA,

10% dextran sulfate, and an oligo-dT probe labeled with digoxigenin at the 3' end. After hybridization, cells were washed three times for 10 min in $2\times$ SSC and incubated with an anti-digoxigenin antibody followed by treatment with an anti-mouse IgG antibody conjugated with FITC.

Immunoprecipitation. The cell extracts were incubated with each primary antibody for 1 h at 4 °C with gentle agitation and with protein A/G-agarose beads (Santa Cruz) for another 1 h. After the agarose pellets had been washed three times with IP buffer, the bound proteins were extracted with SDS-PAGE loading buffer by heating at 95 °C for 5 min and subjected to western blotting.

In vitro and in vivo kinase assay. See **Supplementary Methods** for experimental procedures.

FR901464 and spliceostatin A stability assay. See **Supplementary Methods** for experimental procedures.

NMD assay. See **Supplementary Methods** for experimental procedures.

Note: Supplementary information and chemical compound information is available on the Nature Chemical Biology website.

ACKNOWLEDGMENTS

We thank A. Krainer (Cold Spring Harbor Laboratory) for pSP64-H β A6 and p μ C3-C4, K. Nagata for kind advice regarding preparation of nuclear extracts, and A. Kulozik (University of Heidelberg) for the NMD detection system. We are grateful to the RIKEN Brain Science Institute's Research Resources Center for DNA sequencing analysis and mass spectrometry. This work was supported in part by the CREST Research Project, the Japan Science and Technology Agency, The Strategic Research Programs for R&D, RIKEN, and a Grant-in-Aid from the Ministry of Education, Culture, Sports, Science and Technology of Japan. SF3b image in Graphical Abstract from Golas *et al. Science* **300**, 980–984 (2003). Reprinted with permission from AAAS.

AUTHOR CONTRIBUTIONS

M.Y. is responsible for project planning and experimental design, with support from M.H., T.T. and S.H.; D.K. performed most of the experiments; H.M., K.I., H.W. and T.K. synthesized chemical compounds; E.T. carried out *in vitro* kinase assays; T.N. performed *in vitro* splicing assays; T.Y. carried out pilot study; H.N. prepared FR901464.

COMPETING INTERESTS STATEMENT

The authors declare no competing financial interests.

Published online at <http://www.nature.com/naturechemicalbiology>

Reprints and permissions information is available online at <http://npg.nature.com/reprintsandpermissions>

- Kramer, A. The structure and function of proteins involved in mammalian pre-mRNA splicing. *Annu. Rev. Biochem.* **65**, 367–409 (1996).
- Padgett, R.A., Konarska, M.M., Grabowski, P.J., Hardy, S.F. & Sharp, P.A. Lariat RNA's as intermediates and products in the splicing of messenger RNA precursors. *Science* **225**, 898–903 (1984).
- Ruskin, B., Krainer, A.R., Maniatis, T. & Green, M.R. Excision of an intact intron as a novel lariat structure during pre-mRNA splicing *in vitro*. *Cell* **38**, 317–331 (1984).
- Nagai, K. *et al.* Structure and assembly of the spliceosomal snRNPs. Novartis Medal Lecture. *Biochem. Soc. Trans.* **29**, 15–26 (2001).
- Black, D.L., Chabot, B. & Steitz, J.A. U2 as well as U1 small nuclear ribonucleoproteins are involved in premessenger RNA splicing. *Cell* **42**, 737–750 (1985).
- Mount, S.M., Pettersson, I., Hinterberger, M., Karmas, A. & Steitz, J.A. The U1 small nuclear RNA-protein complex selectively binds a 5' splice site *in vitro*. *Cell* **33**, 509–518 (1983).
- Berglund, J.A., Chua, K., Abovich, N., Reed, R. & Rosbash, M. The splicing factor BBP interacts specifically with the pre-mRNA branchpoint sequence UACUAAC. *Cell* **89**, 781–787 (1997).
- Zamore, P.D. & Green, M.R. Identification, purification, and biochemical characterization of U2 small nuclear ribonucleoprotein auxiliary factor. *Proc. Natl. Acad. Sci. USA* **86**, 9243–9247 (1989).
- Gozani, O., Potashkin, J. & Reed, R. A potential role for U2AF-SAP 155 interactions in recruiting U2 snRNP to the branch site. *Mol. Cell. Biol.* **18**, 4752–4760 (1998).
- Konarska, M.M. & Sharp, P.A. Interactions between small nuclear ribonucleoprotein particles in formation of spliceosomes. *Cell* **49**, 763–774 (1987).
- Pikielny, C.W., Rymond, B.C. & Rosbash, M. Electrophoresis of ribonucleoproteins reveals an ordered assembly pathway of yeast splicing complexes. *Nature* **324**, 341–345 (1986).
- Rutz, B. & Seraphin, B. Transient interaction of BBP/ScSF1 and Mud2 with the splicing machinery affects the kinetics of spliceosome assembly. *RNA* **5**, 819–831 (1999).
- Staley, J.P. & Guthrie, C. Mechanical devices of the spliceosome: motors, clocks, springs, and things. *Cell* **92**, 315–326 (1998).
- Galy, V. *et al.* Nuclear retention of unspliced mRNAs in yeast is mediated by perinuclear Mlp1. *Cell* **116**, 63–73 (2004).
- Maquat, L.E. When cells stop making sense: effects of nonsense codons on RNA metabolism in vertebrate cells. *RNA* **1**, 453–465 (1995).
- Dziembowski, A. *et al.* Proteomic analysis identifies a new complex required for nuclear pre-mRNA retention and splicing. *EMBO J.* **23**, 4847–4856 (2004).
- Wang, Q., He, J., Lynn, B. & Rymond, B.C. Interactions of the yeast SF3b splicing factor. *Mol. Cell. Biol.* **25**, 10745–10754 (2005).
- Nakajima, H. *et al.* New antitumor substances, FR901463, FR901464 and FR901465. I. Taxonomy, fermentation, isolation, physico-chemical properties and biological activities. *J. Antibiot. (Tokyo)* **49**, 1196–1203 (1996).
- Nakajima, H. *et al.* New antitumor substances, FR901463, FR901464 and FR901465. II. Activities against experimental tumors in mice and mechanism of action. *J. Antibiot. (Tokyo)* **49**, 1204–1211 (1996).
- Nakajima, H., Kim, Y.B., Terano, H., Yoshida, M. & Horinouchi, S. FR901228, a potent antitumor antibiotic, is a novel histone deacetylase inhibitor. *Exp. Cell Res.* **241**, 126–133 (1998).
- Malumbres, M. & Barbacid, M. Mammalian cyclin-dependent kinases. *Trends Biochem. Sci.* **30**, 630–641 (2005).
- Harper, J.W., Adami, G.R., Wei, N., Keyomarsi, K. & Elledge, S.J. The p21 Cdk-interacting protein Cip1 is a potent inhibitor of G1 cyclin-dependent kinases. *Cell* **75**, 805–816 (1993).
- Polyak, K. *et al.* Cloning of p27Kip1, a cyclin-dependent kinase inhibitor and a potential mediator of extracellular antimitogenic signals. *Cell* **78**, 59–66 (1994).
- Serrano, M., Hannon, G.J. & Beach, D. A new regulatory motif in cell-cycle control causing specific inhibition of cyclin D/CDK4. *Nature* **366**, 704–707 (1993).
- Pagano, M. *et al.* Role of the ubiquitin-proteasome pathway in regulating abundance of the cyclin-dependent kinase inhibitor p27. *Science* **269**, 682–685 (1995).
- Motoyoshi, H. *et al.* Structure-activity relationship for FR901464: a versatile method for the conversion and preparation of biologically active biotinylated probes. *Biosci. Biotechnol. Biochem.* **68**, 2178–2182 (2004).
- Albert, B.J., Sivaramakrishnan, A., Naka, T., Czaiicki, N.L. & Koide, K. Total syntheses, fragmentation studies, and antitumor/antiproliferative activities of FR901464 and its low picomolar analogue. *J. Am. Chem. Soc.* **129**, 2648–2659 (2007).
- Thompson, C.F., Jamison, T.F. & Jacobsen, E.N. FR901464: total synthesis, proof of structure, and evaluation of synthetic analogues. *J. Am. Chem. Soc.* **123**, 9974–9983 (2001).
- Krainer, A.R., Maniatis, T., Ruskin, B. & Green, M.R. Normal and mutant human beta-globin pre-mRNAs are faithfully and efficiently spliced *in vitro*. *Cell* **36**, 993–1005 (1984).
- Watakabe, A., Inoue, K., Sakamoto, H. & Shimura, Y. A secondary structure at the 3' splice site affects the *in vitro* splicing reaction of mouse immunoglobulin mu chain pre-mRNAs. *Nucleic Acids Res.* **17**, 8159–8169 (1989).
- Reed, R. & Hurt, E. A conserved mRNA export machinery coupled to pre-mRNA splicing. *Cell* **108**, 523–531 (2002).
- O'Keefe, R.T., Mayeda, A., Sadowski, C.L., Krainer, A.R. & Spector, D.L. Disruption of pre-mRNA splicing *in vivo* results in reorganization of splicing factors. *J. Cell Biol.* **124**, 249–260 (1994).
- Misteli, T., Caceres, J.F. & Spector, D.L. The dynamics of a pre-mRNA splicing factor in living cells. *Nature* **387**, 523–527 (1997).
- Tanackovic, G. & Kramer, A. Human splicing factor SF3a, but not SF1, is essential for pre-mRNA splicing *in vivo*. *Mol. Biol. Cell* **16**, 1366–1377 (2005).
- Das, B.K. *et al.* Characterization of a protein complex containing spliceosomal proteins SAPs 49, 130, 145, and 155. *Mol. Cell. Biol.* **19**, 6796–6802 (1999).
- Ishida, N. *et al.* Phosphorylation of p27Kip1 on serine 10 is required for its binding to CRM1 and nuclear export. *J. Biol. Chem.* **277**, 14355–14358 (2002).
- Kudo, N. *et al.* Leptomycin B inhibition of signal-mediated nuclear export by direct binding to CRM1. *Exp. Cell Res.* **242**, 540–547 (1998).
- Reed, R. & Magni, K. A new view of mRNA export: separating the wheat from the chaff. *Nat. Cell Biol.* **3**, E201–E204 (2001).
- Rutz, B. & Seraphin, B. A dual role for BBP/ScSF1 in nuclear pre-mRNA retention and splicing. *EMBO J.* **19**, 1873–1886 (2000).
- Abovich, N. & Rosbash, M. Cross-intron bridging interactions in the yeast commitment complex are conserved in mammals. *Cell* **89**, 403–412 (1997).
- Nagy, E. & Maquat, L.E. A rule for termination-codon position within intron-containing genes: when nonsense affects RNA abundance. *Trends Biochem. Sci.* **23**, 198–199 (1998).
- Maquat, L.E. & Li, X. Mammalian heat shock p70 and histone H4 transcripts, which derive from naturally intronless genes, are immune to nonsense-mediated decay. *RNA* **7**, 445–456 (2001).
- Gehring, N.H., Neu-Yilik, G., Schell, T., Hentze, M.W. & Kulozik, A.E. Y14 and hUpf3b form an NMD-activating complex. *Mol. Cell* **11**, 939–949 (2003).
- Lander, E.S. *et al.* Initial sequencing and analysis of the human genome. *Nature* **409**, 860–921 (2001).
- Montagnoli, A. *et al.* Ubiquitination of p27 is regulated by Cdk-dependent phosphorylation and trimeric complex formation. *Genes Dev.* **13**, 1181–1189 (1999).
- Fukuhara, T. *et al.* Utilization of host SR protein kinases and RNA-splicing machinery during viral replication. *Proc. Natl. Acad. Sci. USA* **103**, 11329–11333 (2006).
- Hamamoto, T., Gunji, S., Tsuji, H. & Beppu, T. Leptomycins A and B, new antifungal antibiotics. I. Taxonomy of the producing strain and their fermentation, purification and characterization. *J. Antibiot. (Tokyo)* **36**, 639–645 (1983).
- Dignam, J.D., Lebovitz, R.M. & Roeder, R.G. Accurate transcription initiation by RNA polymerase II in a soluble extract from isolated mammalian nuclei. *Nucleic Acids Res.* **11**, 1475–1489 (1983).